Journal of Management Science and Engineering 10 (2025) 245–261

Contents lists available at ScienceDirect

Journal of Management Science and Engineering

journal homepage: www.keaipublishing.com/en/journals/journal-of-management-science-and-engineering/

Early warning of bubbles in the agricultural commodity market: Evidence from LPPLS confidence indicators

Hai-Chuan Xu [a, b], Yu-Zhen Tan [a], Han-Xiao Fan [a], Wei-Xing Zhou [a, b, *]

[a] School of Business, East China University of Science and Technology, Shanghai, 200237, China
[b] Research Center for Econophysics, East China University of Science and Technology, Shanghai, 200237, China

ARTICLE INFO

Article history:
Received 20 May 2024
Received in revised form 9 December 2024
Accepted 18 January 2025
Available online 8 March 2025

Keywords:
Bubbles
Early warning
LPPLS
Agricultural commodities

ABSTRACT

This study leverages the Log-Periodic Power Law Singularity (LPPLS) confidence indicator to effectively identify bubbles in agricultural commodity markets. We analyze five major grain price indices reported by the International Grains Council (IGC) from January 2000 to April 2023, successfully identifying several notable bubble periods. These include a positive bubble in 2004 driven by decreased food production, a substantial positive bubble during the 2008 global financial crisis, a negative bubble in 2016, and positive bubbles triggered by the COVID-19 pandemic and the Russo-Ukrainian conflict since 2020. As the critical point is approached, the LPPLS confidence indicator exhibits strong early warning capabilities. To verify the model's robustness, we employ the Bai-Perron test for multiple structural breaks, detecting five such breaks in each agricultural commodity price series. LPPLS indicators provide strong early-warning signals prior to these break dates. Finally, we investigate the predictability of price bubbles in the agricultural commodity market. Using a Markov regime-switching model, our findings confirm that the geopolitical risk index possesses significant predictive power for bubble formation.

1. Introduction

The stability of agricultural commodity markets is crucial for global food security and has attracted increasing attention. The 2008 financial crisis triggered a sustained escalation in global agricultural prices, leading to a severe global food crisis. This resulted in a sharp decline in food imports in regions such as North Africa, exacerbating hunger and intensifying social conflicts. The unexpected outbreak of the COVID-19 pandemic in 2020 further disrupted global supply chains, impacting agricultural commodity trade and causing food prices to soar. Consequently, supply chains were disrupted, agricultural commodity imports and exports plummeted, and food prices skyrocketed. The conflict between Russia, a major grain exporter, and Ukraine, a relevant wheat exporter, in early 2022 delivered another shock to the global agricultural system, driving wheat prices to a 14-year high.

Price booms and collapses in agricultural markets can lead to the formation and bursting of bubbles, posing substantial risks to market participants and economic stability. Therefore, developing an early-warning indicator capable of accurately identifying agricultural price bubbles is crucial. Such a tool would aid in monitoring market risks, formulating effective policy

* Corresponding author.
E-mail address: wxzhou@ecust.edu.cn (W.-X. Zhou).

https://doi.org/10.1016/j.jmse.2025.01.002

measures, and guiding market participants' decision-making. By identifying bubbles in advance and limiting their expansion, potential losses can be mitigated. The Food and Agriculture Organization of the United Nations (FAO) proposes a tool called compound growth rate for early warning on agricultural price, which categorizes agricultural price into states of normal, vigilance and early warning, issuing alerts when the indicator value exceeds a certain threshold. However, its performance is not perfect as the indicator may erroneously issue an early warning or fail to issue an alert when necessary (Baquedano, 2015).

This study utilizes the Log-Periodic Power Law Singularity (LPPLS) model to detect bubble states in five grain price indices reported daily by the International Grains Council (IGC) (Johansen et al., 2000). Initially applied to earthquake monitoring, the LPPLS model has been successfully generalized to monitor financial market bubbles. The LPPLS confidence indicator serves as a statistical index to assess the degree of conformity of time series data to bubble characteristics; this is achieved by fitting the LPPLS model across various time windows (Demirer et al., 2019).

Our contributions are twofold. First, we examine the feasibility and robustness of the LPPLS confidence indicator as an early-warning signal for agricultural bubbles. Unlike other bubble diagnostic methods, such as the Generalized Supremum Augmented Dickey-Fuller (GSADF) (Phillips et al., 2015) and Bai-Perron (Bai and Perron, 2006) tests, which require the use of the entire sample to detect the presence of bubbles over a period of time or whether a certain point in time is a breakpoint. The LPPLS confidence indicator only uses historical data pr ior to the current moment, enabling true early warning. Second, we investigate the role of several global macroeconomic uncertainties in agricultural bubble formation, confirming the driving role of these uncertainties, especially geopolitical risk.

Specifically, we use the LPPLS confidence index to effectively identify multiple positive and negative bubbles in the global agricultural market from January 2000 to April 2023, including a positive bubble caused by reduced grain production in 2004, a major positive bubble during the 2008 global financial crisis, a negative bubble in 2016, and positive bubbles stemming from the COVID-19 and the Russo-Ukrainian war.

We implement stringent filtering conditions for the LPPLS method to enhance the robustness of the confidence indicator. Our findings demonstrate a degree of consistency between the bubbles identified by the LPPLS confidence index and the multiple structural breaks detected by the Bai-Perron test, with the former exhibiting a distinct forward-looking characteristic. Importantly, the LPPLS confidence index allows for real-time bubble detection and warning issuance.

Finally, we investigate the predictability of price bubbles in agricultural commodities. We employ a Markov switching model to assess the effectiveness of the geopolitical risk index in predicting bubble indicators within the international agricultural market, offering valuable insights into market price warnings from a macro uncertainty perspective.

2. Literature review

2.1. The bubbles of agricultural commodities

The 2008 surge in grain prices sparked considerable research into the existence of price bubbles in agricultural commodity markets. Piesse and Thirtle (2009) identify bubbles in soybean, wheat, and maize prices during 2007–2008, alongside a rice price "panic", while Headey and Fan (2008) characterize the rice price spikes as "almost entirely a bubble". Gutierrez (2013) employs bootstrap methods and Monte Carlo simulations, finding evidence of bubble collapses in wheat, maize, and brown rice, but minimal evidence for soybeans. Adämmer and Bohl (2015) further confirm the presence of bubbles in the US wheat market using a momentum threshold autoregressive (MTAR) model. Etienne et al. (2014) apply new bubble tests to commodity futures prices, finding evidence of explosiveness in some agricultural markets (wheat, corn, and rice) but not in others. This suggests that while bubbles may exist, they are not universal across all agricultural commodities. Brooks et al. (2015) extend this analysis to a broader range of commodities and a longer timeframe, finding evidence for bubbles only in crude oil and feeder cattle markets. Their work emphasizes the importance of using individual futures contract prices—less influenced by fundamental supply and demand factors—to identify speculative behavior. These studies focus primarily on the 2008 period and lack generalized approaches to bubble detection and early-warning systems.

The role of speculation in driving commodity price bubbles is a central point of contention. Some researchers, such as Timmer (2010), attribute the 2007–2008 grain price surge to a speculative bubble fueled by market inflows, particularly from commodity index traders prioritizing portfolio diversification over market fundamentals (Basak and Pavlova, 2016). However, other studies, such as that of Etienne et al. (2015), challenge the notion that speculation alone explains the price increases. Sanders and Irwin (2017) address methodological criticisms of earlier studies, such as the low power of time-series tests and omission of conditioning variables. Using updated data and new empirical approaches, including cross-sectional regressions and examinations of extreme price movements, they find little support for the "Masters Hypothesis", which posits a substantial impact of index funds on commodity prices.

More recent studies focus on specific markets and refined methodologies. Li et al. (2017) explore the link between commodity price bubbles and macroeconomic factors in Chinese agricultural markets, finding that economic growth, money supply, and inflation positively affect bubble occurrences, while interest rates have a negative effect. Huang and Xiong (2020) examine price bubbles and market integration in global sugar futures markets, finding evidence of bubbles and increased market integration during these periods. Akyildirim et al. (2022) investigate the connectedness between agricultural commodity futures markets and news-based investor sentiment, highlighting the influence of economic and financial uncertainties, including the COVID-19 pandemic. Chen et al. (2023) provide evidence of price bubbles in China's agricultural futures market—particularly in soybeans—and discuss the impact of agricultural policy reforms on bubble formation. Mao et al. (2021)

identify bubble dates in China's maize and soybean futures markets using the GSADF test and wild bootstrap procedure. Fang et al. (2023) explore the predictability of price bubbles in Chinese agricultural commodity futures using the LPPLS model, highlighting the influence of investor sentiment and macroeconomic factors. Yang et al. (2024) investigate the relationship between monetary policy uncertainty and price bubbles in U.S. oil futures, revealing a correlation between monetary policy uncertainty peaks and bubble occurrences. Potrykus (2023) examines price bubbles across various commodity sectors, identifying commodities prone to bubbles and the influence of financial crises. Finally, Mao et al. (2024) investigate asynchronous price bubbles in Chinese agricultural futures and spot markets, finding that while futures prices dominate price discovery, spot prices exhibit more frequent bubbles, potentially owing to speculative storage and market power.

While the impact of speculation and index funds on agricultural commodity prices remains debated, the literature suggests that the influence of speculation is likely market-specific and should be considered within the broader context of fundamental market drivers. Methodological advancements and a focus on specific markets and macroeconomic factors are contributing to a more nuanced understanding of price bubble dynamics in commodity markets. However, the existing literature overlooks the role of global macroeconomic factors in the formation of agricultural commodity bubbles, such as geopolitical uncertainty and climate risk, focusing solely on the impact of monetary policy in specific markets, such as China (Fang et al., 2023) or the United States (Yang et al., 2024). Additionally, further research is needed to refine bubble detection methods, explore the interplay of various influencing factors, and develop effective early warning systems to mitigate the potential negative consequences of agricultural commodity price bubbles.

2.2. The diagnostic methods of bubbles

Bubbles are used to characterize the process of an asset's price significantly deviating from its intrinsic value owing to internal or external shocks, leading to market failure and economic depression (Sornette and Cauwels, 2015). This deviation is characterized by a rapid increase in price followed by a subsequent decline, often resulting in market crashes. Shiller (2015) mentions the presence of both positive and negative bubbles in his book *Irrational Exuberance*. A positive bubble occurs when the present value of an asset significantly exceeds its fundamental value owing to excessive demand or overpricing during temporary and unsustainable periods in the markets. Conversely, a negative bubble arises when the fundamental value surpasses the current value as a result of excessive selling during a period of mispricing where most assets are undervalued. Commonly used diagnostic tools for identifying bubbles include the Augmented Dickey-Fuller (ADF)-like and LPPLS models. This paper provides a comprehensive review of these two types of models.

The SADF (Supremum Augmented Dickey-Fuller) method represents an improvement of the classic ADF approach, enhancing the bubble detection capability by incorporating right-tailed unit root and positive recursive regression based on a simple ADF test. Therefore, it offers more precise critical values for detecting unit roots in time series data (Phillips and Magdalinos, 2007; Phillips et al., 2010, 2011). The SADF model utilizes a sliding window approach to calculate ADF statistics, providing more accurate results for determining the existence of a unit root and estimating the smoothness of time series data. When the maximum value of the ADF statistic as the SADF statistic is selected, its highest value can be captured even when lag order is uncertain. The unit root's explosive behavior is then examined by comparing the corresponding right-tail critical values derived from both the recursive and standard ADF statistics to ascertain the presence of a unit root and its nonstationarity. Rejection of the unit root hypothesis can be inferred if the SADF statistic exceeds the critical value, which suggests that nonstationarity and price bubbles may exist in time series, and the initiation and collapse dates of the bubble phase can be predicted.

In light of the frequent periodic bubbles and bursts in the markets, Phillips et al. (2015) make modifications to the SADF statistic and propose the GSADF test, which not only improves the performance of the SADF test but also effectively increases its ability to detect bubbles and bursts. By introducing volatility estimates and adjustment terms, the GSADF test aims to correct the SADF statistic to improve reliability and accuracy. To account for volatile price changes during bubble formation, the GSADF model utilizes a Heterogeneous Autoregressive (HAR) model for estimating asset price volatility and captures long-term fluctuation characteristics using a relatively extended time window. To eliminate estimation bias and correct the impact of volatility estimates, the GSADF model incorporates an adjustment term to enhance the robustness of the GSADF statistic. The selection of this term is typically based on experience or alternative statistical methods. Since the distribution of the GSADF statistic does not conform to classical statistical theory, simple methods for computing its critical value are not available. Hence, the model employs either a hypothetical simulation based on random walk or Monte Carlo method to calculate the critical value of the GSADF statistic. If the GSADF statistic surpasses this critical value, it indicates nonstationarity in asset prices and potential existence of bubbles. Furthermore, the GSADF model can measure the intensity and evolutionary process of bubbles. Conducting sliding window analysis on asset price time series allows for computing GSADF statistics for various time periods and observing their dynamic trends. A higher GSADF value indicates a heightened likelihood of bubble presence, while fluctuations in the GSADF value can signify the developmental stages of market bubbles, including their formation, expansion, and collapse. Moreover, the GSADF model can be applied in predicting bubble development and managing market risks. The analysis of historical data using GSADF can identify patterns related to bubble formation and collapse, thus facilitating prediction regarding market risk conditions.

The LPPLS model, also referred to as the JLS (Johansen-Ledoit-Sornette) model, utilizes critical points adjusted by log-periodic functions to detect stock market bubbles (Johansen et al., 2000). The model proposes that during periods of herding behavior in the market, a group of traders imitating each other emerges. This imitation behavior, reinforced by the internal system's positive feedback mechanism, leads to gradual asset price bubble formation and eventual collapse. As the bubble approaches its bursting point, asset prices exhibit log-periodic power law characteristics (Sornette, 2009).

The LPPLS model can be applied to identify whether an asset market is in a bubble state and provide advance warning of the bubble's bursting point when the broader market peaks (Johansen et al., 2000; Sornette et al., 2015; Abreu and Brunnermeier, 2003; Demos and Sornette, 2017). It is primarily used to monitor endogenous crashes, with limited application in detecting exogenous crashes. In endogenous crashes, the model is based on the super-exponential growth of price trajectories. When financial bubbles are amplified by herd and noise behavior, the interactions among market participants involve long-memory processes. For instance, Bartolozzi et al. (2005) analyze the time series data of the DAX, Nasdaq 100, S&P 500, and Dow Jones indexes from 2000 to 2004. Their study reveals that the index exhibits sustained log-periodic oscillations for approximately two years starting from September 2000, thereby characterizing discrete scale invariance within this complex system. Additionally, Zhou and Sornette (2004) pioneer the application of the LPPLS model in analyzing China's stock market bubbles. Their prediction indicates that the Chinese A-share market would reach the bottom in 2003 and then rebound at the beginning of the following year. Subsequent results validate the strong predictive capability of the LPPLS model for asset price bubbles. Jiang et al. (2010) utilize the LPPLS model to identify asset price bubbles in Shanghai Stock Exchange composite index and Shenzhen Stock Exchange composite index from May 2005 to July 2009 in China and successfully anticipate the time windows of both crashes. In a separate study, Zhi et al. (2019) conduct a series of bubble diagnostic analysis over 35 representative cities in China using the LPPLS model, emphasizing the importance of bubble diagnostic tests tailored to specific bubble characteristics.

In recent years, the LPPLS model has undergone continuous revision and improvement. Filimonov and Sornette (2013) revise the LPPLS formula by compressing the number of nonlinear parameters in the function from four to three, thus reducing the calibration complexity. Lin et al. (2014) develop a self-consistent model for identifying explosive financial bubbles and diagnosing their duration. Additionally, Filimonov et al. (2017) utilize improved contour likelihood estimation to calibrate the LPPLS model, thus obtaining interval estimates of critical times. Furthermore, Demirer et al. (2019) propose multi-scale LPPLS confidence indicators. Their application to the S&P500, FTSE and Nikkei indices demonstrates that the LPPLS framework can effectively capture prominent bubbles across various time scales.

3. Data and method

3.1. Data

We select all grain price index data from January 2000 to April 2023, provided by the International Grains Council (IGC), encompassing rice, wheat, soybeans, barley and maize. Each price index is based on daily quotes from multiple official and trade sources. These five crops are the primary source of caloric intake for the global population and hold critical importance in the agricultural market. To investigate the global macroeconomic drivers of price bubbles, we also collect the geopolitical risk index developed by Caldara and Iacoviello (2022) and transition and physical climate risk indices, developed by Bua et al. (2024).

3.2. The LPPLS model

In the bubble regimes, Johansen et al. (2000) assume that the logarithm of observable asset prices $p(t)$ can be expressed as follows:

$$\frac{\mathrm{d}p}{p} = \mu(t)\mathrm{d}t + \sigma(t)dW - kdj, \tag{1}$$

where $\mu(t)$ is the expected return; $\sigma(t)$ is the volatility; dW is an infinitesimal increment of the standard Wiener process; k quantifies the magnitude of a possible crash, and dj represents a discontinuous jump where $j = n$ before and $j = n + 1$ after the crash (with n being an integer).

Assuming that $h(t)\mathrm{d}t$ refers to the likelihood of a crash occurring within the time interval of t and $t + \mathrm{d}t$, that is, the crash hazard rate, the following can be obtained (Johansen et al., 2000):

$$E[dj] = 1 \times h(t)\mathrm{d}t + 0 \times (1 - h(t))\mathrm{d}t = h(t)\mathrm{d}t. \tag{2}$$

The model considers two types of subjects: the first group comprises traders with rational expectations, while the second group consists of noise traders who tend to exhibit herd behavior. The assumption is that the collective actions of these latter individuals can destabilize asset prices through correlated transactions. Johansen et al. (2000) propose that their behavior can be measured by formulating the crash hazard rate as follows:

$$h(t) = \alpha(t_c - t)^{m-1}(1 + \beta\cos(\omega\ln(t_c - t) - \varphi'), \tag{3}$$

with α, β, ω and t_c are parameters. The above formula shows that the risk of crash resulting from herd behavior is the sum of power law singularities $\alpha(t_c - t)^{m-1}$, which are modulated by oscillations of varying amplitudes whose period is the logarithm of the critical time t_c. Seyrich and Sornette (2016)'s percolation model provides a microscopic basis for this behavior. The economic principles and research framework underlying this article can be traced back to Lux (1995)'s proposition that uninformed and unsophisticated traders can be infected by market sentiment (either optimistic or pessimistic) and consequently engage in trading. Hüsler et al. (2013)'s experiments and Leiss et al. (2015)'s empirical study on implied risk premium demonstrate that during bubbles, power law singularities indicate faster price growth than exponential growth. The accelerated log-periodic oscillations captured by $\beta\cos(\bullet)$ is dynamically driven by the structure of social hierarchies, ranging from the state to banks, internal organizations, trading blocs, and finally to individual traders.

The no-arbitrage condition requires that the excess return $\mu(t)$ during the bubble stage is directly proportional to the crash hazard rate given by Eq. (3). In fact, by setting $E[dp] = 0$ and assuming that the risk has not yet occurred ($dj = 0$), in conjunction with Eq. (2), we can derive:

$$\mu = kh(t). \tag{4}$$

Hence, under no-arbitrage condition, excess returns can be determined by the crash hazard rate.

By integration, we obtain the expected logarithm of prices during the bubble stage before the crash occurs:

$$E[\ln p(t)] = A + B|t_c - t|^m + C|t_c - t|^m\cos(\omega\ln|t_c - t| - \varphi), \tag{5}$$

where $B = -k\alpha/m$ and $C = -k\alpha\beta/\sqrt{m^2+\omega^2}$. Among them, $A > 0$ represents the price that $p(t)$ would reach if the bubble persisted until a critical time t_c; $B < 0$ signifies the upward acceleration process of price; parameter C quantifies logarithmic periodic fluctuations, serving as a measure of the amplitude of fluctuations around the index; $t_c > 0$ denotes the critical time for the bubble to burst and the time point when the environment of asset prices is most likely to change; $t < t_c$ refers to the time point prior to the bubble bursting; $0 < m < 1$ measures the acceleration of price increases; ω is the angular frequency of price fluctuations during the bubble, and $0 < \varphi < 2\pi$ represents the initial phase of cyclical fluctuations. The term $B(t_c - t)^m$ describes the process of superpower exponential growth, with accelerated price increases driven by a positive feedback mechanism. The periodic term $C(t_c - t)^m\cos(\omega\ln(t_c - t) - \varphi)$ corrects for superexponential behavior.

The general characteristics of the positive bubble regimes are $0 < m < 1$ and $B < 0$, while those of the negative bubble regimes are $B > 0$. The inequality $m < 1$ is utilized to depict the super-exponential growth in price as time approaches t_c, while $0 < m$ ensures that the probability of a crash (controlled by the integral of the hazard rate) is limited. Finally, considering that the hazard rate $h(t)$ is nonnegative, we can transform the above inequalities into the constraint $D = m|B|/\omega|C| > 1$, where D represents a *damping* parameter.

3.3. Model estimation

The model contains four nonlinear parameters and three linear parameters. Following the approach of Filimonov and Sornette (2013), we substitute the two parameters C and φ in the original formula with two linear parameters $C_1 = C\cos\varphi$ and $C_2 = C\sin\varphi$. This modification reduces the nonlinear parameter set from four elements (m, ω, t_c, φ) to three elements (m, ω, t_c), while re-expressing the linear parameter set as (A, B, C_1, C_2), thus simplifying the calibration complexity of the LPPLS model. Therefore, we can rewrite Eq. (5) as:

$$\ln p(t) = A + B(t_c - t)^m + C_1(t_c - t)^m\cos(\omega\ln(t_c - t)) + C_2(t_c - t)^m\sin(\omega\ln(t_c - t)). \tag{6}$$

We estimate the parameter set $S = \{A, B, C_1, C_2, m, \omega, t_c\}$ by minimizing the N-dimensional distance between the real and the theoretical values. Using the least square method, we set the objective function as:

$$F(A, B, C_1, C_2, m, \omega, t_c) = \sum_{i=1}^{N}[\ln[p(t_i)] - A - B(f_i) - C_1(g_i) - C_2(h_i)]^2, \tag{7}$$

where,

$$f_i \equiv (t_c - t_i)^m, \tag{8}$$

$$g_i \equiv (t_c - t_i)^m\cos(\omega\ln(t_c - t_i)), \tag{9}$$

$$h_i \equiv (t_c - t_i)^m\sin(\omega\ln(t_c - t_i)), \tag{10}$$

and then,

$$\{\widehat{A}, \widehat{B}, \widehat{C_1}, \widehat{C_2}, \widehat{m}, \widehat{\omega}, \widehat{t_c}\} = \underbrace{\arg\min}_{A,B,C_1,C_2,m,\omega,t_c} F(A,B,C_1,C_2,m,\omega,t_c). \tag{11}$$

We proceed in two steps. First, we slave the linear parameters $\{A, B, C_1, C_2\}$ to the remaining nonlinear parameters $\{m, \omega, t_c\}$ by solving the following matrix equations

$$\begin{bmatrix} N & \sum f_i & \sum g_i & \sum h_i \\ \sum f_i & \sum f_i^2 & \sum f_i g_i & \sum f_i h_i \\ \sum g_i & \sum f_i g_i & \sum g_i^2 & \sum g_i h_i \\ \sum h_i & \sum f_i h_i & \sum g_i h_i & \sum h_i^2 \end{bmatrix} \begin{bmatrix} \widehat{A} \\ \widehat{B} \\ \widehat{C_1} \\ \widehat{C_2} \end{bmatrix} = \begin{bmatrix} \sum y_i \\ \sum y_i f_i \\ \sum y_i g_i \\ \sum y_i h_i \end{bmatrix} \tag{12}$$

Second, we estimate the nonlinear parameters $\{m, \omega, t_c\}$ by

$$\{\widehat{m}, \widehat{\omega}, \widehat{t_c}\} = \underbrace{\arg\min}_{m,\omega,t_c} F_1(m,\omega,t_c). \tag{13}$$

Using these calculations, we can derive all the relevant parameters. Fig. 1 illustrates the LPPLS fitting results of wheat and barley price indices during a bubble period. We use 470 days of price time series from June 25, 2020 to April 14, 2022 for fitting. The corresponding parameter estimates are presented in Table 1.

Owing to the impact of the COVID-19 pandemic and Russo-Ukrainian war in 2022, wheat and barley prices experienced a sustained rise. The LPPLS model predicts a critical point for the wheat price index on May 5, 2022. The actual peak occurred on May 17, 2022, resulting in a time error of 12 days. For barley, the model predicts a bubble burst on April 17, 2022, while the actual peak and burst occurred on May 18, 2022, with a time error of 29 days. These results demonstrate that the LPPLS model can effectively detect bubbles in real-time and predict their bursting point before they occur.

3.4. *The LPPLS confidence indicator*

The above estimates, derived from an arbitrarily chosen time window, lack robustness. To assess the reliability of bubble warning indicators, testing whether the time series exhibits bubble characteristics across multiple time windows is necessary. We introduce the LPPLS confidence indicator, defined as the proportion of time windows that conform to the LPPLS bubble structure. Following the approach of Demirer et al. (2019), we identify estimates that satisfy the filtering conditions as indicative of bubble characteristics. Table 2 provides the search space and filter conditions for LPPLS fits, which are well-established empirical settings. When the confidence index is close to 1, the LPPLS pattern exists across nearly all time windows, suggesting higher reliability. Conversely, a low confidence index implies that the signal may be weak as it only appears within a limited number of suitable windows. Let t_2 represent the end time of the time window, which can also be considered the nearest time point for model estimation. We define $[t_1: t_2]$ as the fitting time window, where t_2 is fixed and t_1 is determined by the number of days in the selected time window. In our empirical analysis, we select 691 windows, ranging from 30 days to 720 days as our chosen time window.

4. Empirical results

4.1. *Bubble diagnosis of five agricultural commodities*

Figs. 2-6 depict the fluctuations in the bubble confidence indicator values for these five agricultural commodities. The black curve represents the logarithmic price of agricultural commodities, while the red and green curves signify the confidence indicator values for positive and negative bubbles, respectively.

4.1.1. *Wheat*

Fig. 2 shows the bubble state of the wheat price index. We observe distinct positive bubble clusters from April 2006 to April 2008, October 2010 to March 2011, and May 2021 to July 2022, as well as noticeable negative bubble clusters from July 2008 to August 2009 and June 2014 to January 2017. During this period, the wheat price index surges from 130 in March 2006 to 450 in February 2008, an increase of 246 % in two years. Subsequently, it experiences a sharp decline to reach a low of 184 in November 2008, a decrease of 59 %. This trend of rapid ascent followed by steep descent is effectively captured by the LPPLS confidence indicator. As the LPPLS pattern appears regularly within this time window with sufficiently large indicator values, it enables highly accurate predictions and judgments regarding bubble formation. In 2011, we observe a significant wheat price rebound, with the positive bubble confidence indicators consistently issuing early alerts. This can be attributed to the escalating fertilizer and pesticide prices since 2010, which results in increased wheat cultivation costs, and extreme weather

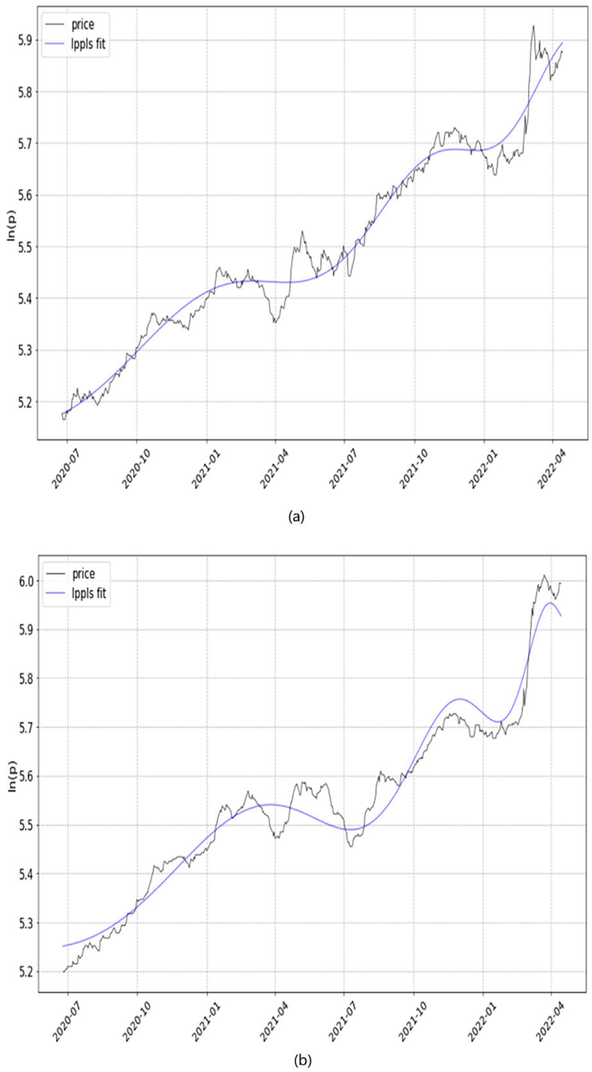

Fig. 1. LPPLS fitting curves of wheat price index and barley price indices from June 25, 2020 to April 14, 2022.

Table 1
Fitting parameter values of wheat price index and barley price index from June 25, 2020 to April 14, 2022.

	t_c	m	ω	A	B	C_1	C_2
wheat	2022/5/5	0.08219	5.08656	7.47452	−1.20198	0.02080	0.04516
barley	2022/4/17	0.47681	2.58727	6.07839	−0.03262	−0.00284	−0.01697

Table 2
Search space and filter conditions for the valid LPPLS fits.

Item	Notation	Search space	Filter condition
3 nonlinear parameters	m	[0, 2]	[0.01, 0.99]
	ω	[2, 25]	[2, 15]
	t_c	$[t_2 - 0.5\mathrm{d}t, t_2 + 0.5\mathrm{d}t]$	$[t_2 - 0.05\mathrm{d}t, t_2 + 0.1\mathrm{d}t]$
Number of oscillations	$\frac{\omega}{2}\ln\left\lvert\frac{t_c - t_1}{t_c - t_2}\right\rvert$	–	$[2.5, +\infty]$
Damping	$\frac{m\lvert B\rvert}{\omega\lvert C\rvert}$	–	$[1, +\infty]$
Relative error	$\frac{P_t - \widehat{P}_t}{P_t}$	–	[0, 0.2]

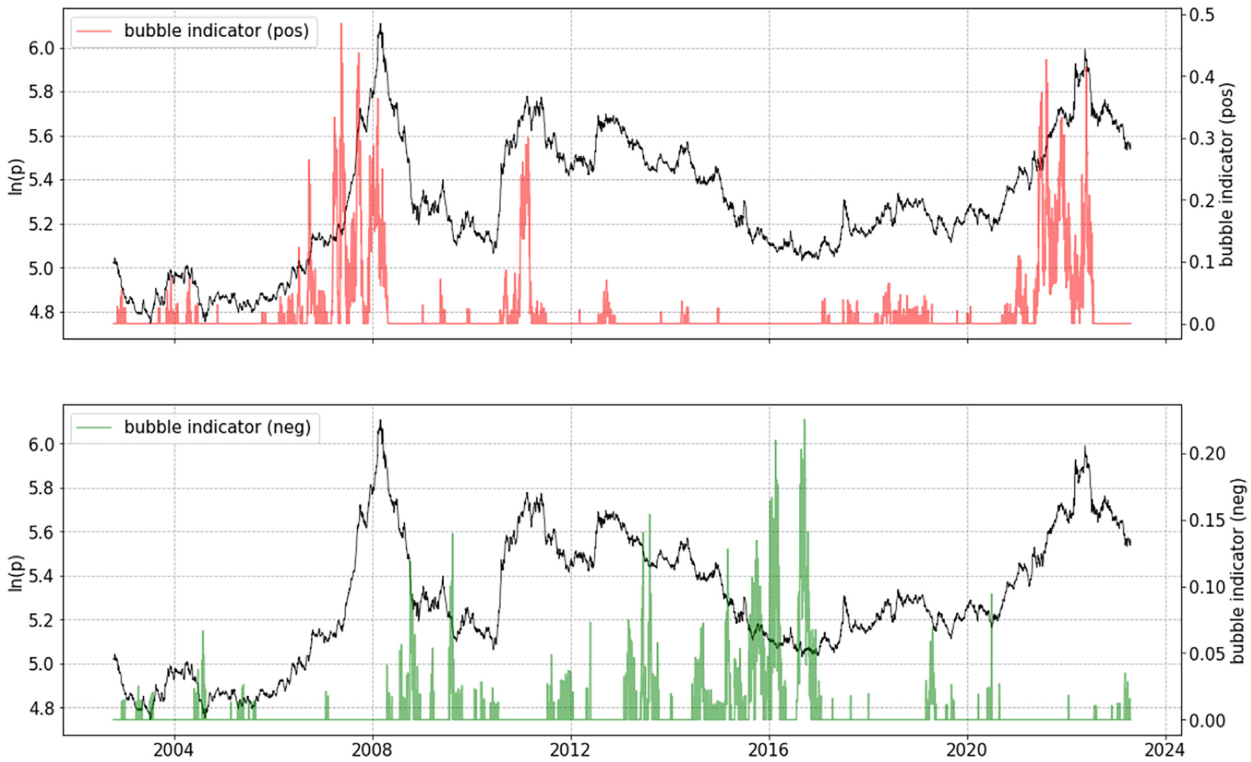

Fig. 2. LPPLS bubble confidence indicators of wheat price index.
LPPLS confidence indicators for positive bubbles (upper panel) and negative bubbles (lower panel). The continuous black line indicates the logarithmic price of wheat from January 2000 to April 2023; the red one represents a positive bubble indicator, and the green one denotes a negative bubble indicator.

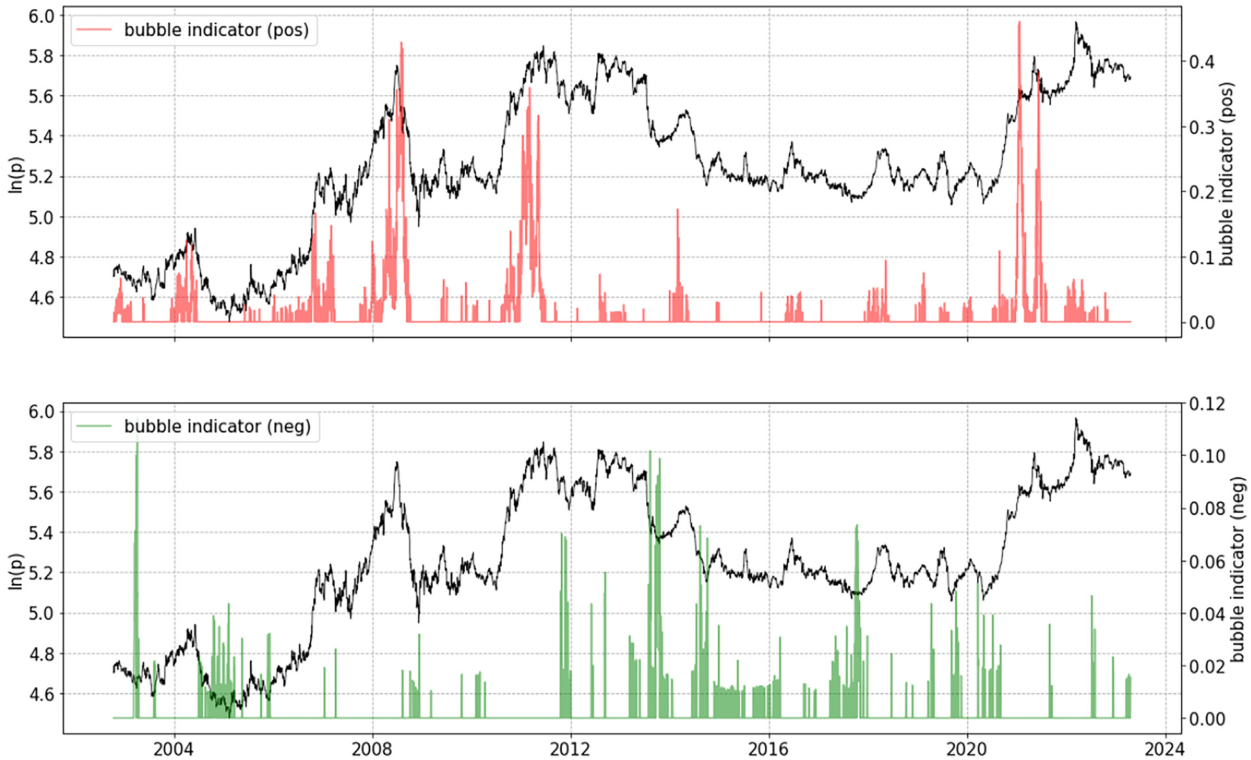

Fig. 3. LPPLS bubble confidence indicators of maize price index.
LPPLS confidence indicators for positive bubbles (upper panel) and negative bubbles (lower panel). The continuous black line indicates the logarithmic price of maize from January 2000 to April 2023; the red one represents a positive bubble indicator, and the green one denotes a negative bubble indicator.

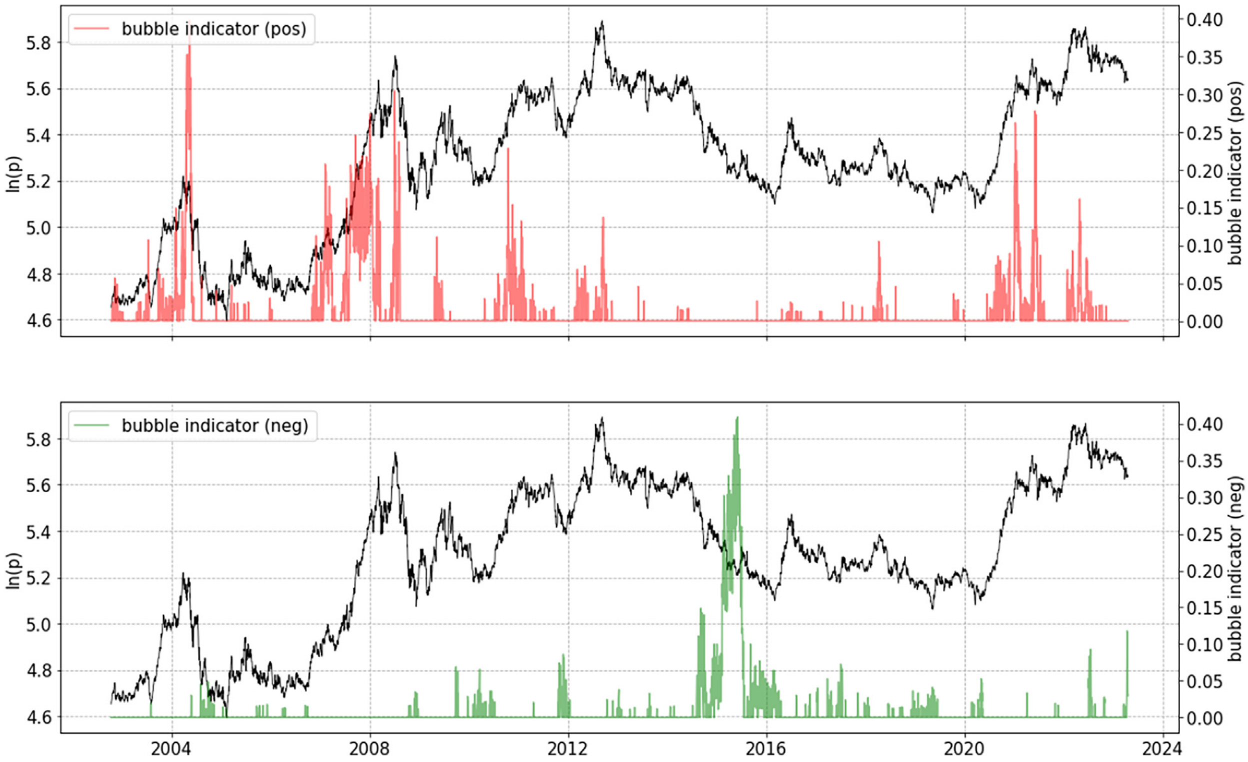

Fig. 4. LPPLS bubble confidence indicators of soybeans price index.
LPPLS confidence indicators for positive bubbles (upper panel) and negative bubbles (lower panel). The continuous black line indicates the logarithmic price of soybeans from January 2000 to April 2023; the red one represents a positive bubble indicator, and the green one denotes a negative bubble indicator.

conditions such as severe drought in the United States, which causes diminished international wheat production. From November 2012 to September 2016, the wheat price index experiences a consecutive annual decline from 296 to 155, a decrease of 48 %. The negative bubble indicators begin to issue warnings from the beginning of this continuous downward trend, with stronger warnings observed closer to the lowest point. The impact of COVID-19 since 2020 leads to a gradual upward trend in the wheat price index, while the Russo-Ukrainian war in 2022 pushes the price index to its peak. In this regard, the confidence indicators detect significant positive bubble characteristics.

4.1.2. Maize

The bubble state of the maize price index is depicted in Fig. 3. We observe positive bubble clusters from December 2007 to September 2008, December 2010 to June 2011, and May 2021 to July 2022. Moments with higher confidence in negative bubbles tend to occur around the bottom of the price index. Overall, both positive and negative bubble indicators can capture the abnormal behavior of maize prices relatively well.

4.1.3. Soybeans

Fig. 4 illustrates the bubble state observed in the soybeans price index. We observe remarkable positive bubble clusters from September 2003 to June 2004, May 2007 to March 2008, and December 2020 to July 2022, in addition to successive waves of positive bubble clusters from September 2010 to February 2011 and April 2012 to October 2012. We find significant negative bubble clusters from August 2014 to July 2015. Specifically, the highest growth in the crop in the vicinity of 2004 is seen in the soybeans price index, which increases by 128 % from 81 in February 2002 to 185 in March 2004. Simultaneously, positive bubble indicators send a strong signal. During the 2008 financial crisis, the soybean price index climbs by 188 %, from 108 in April 2006 to 311 in July 2008. The figure shows that the signals from the positive bubble indicators become increasingly stronger as they approach the maximum point of the price index, which indicates the reliability of the results. From 2012 to 2016, the soybean price index falls year by year. Strong negative bubble signals are issued in late 2014 and early 2015, with a maximum value of more than 0.4. After 2020, similar to wheat and maize, the price index of soybeans continues to rise owing to the impact of COVID-19, and then governments introduce policies to regulate the issue, which makes the price fall slightly. However, the outbreak of the Russo-Ukrainian war brings food prices to an urgent level again. Like the maize price index, the positive bubble signals are particularly strong when the soybean price index reaches its first minor peak.

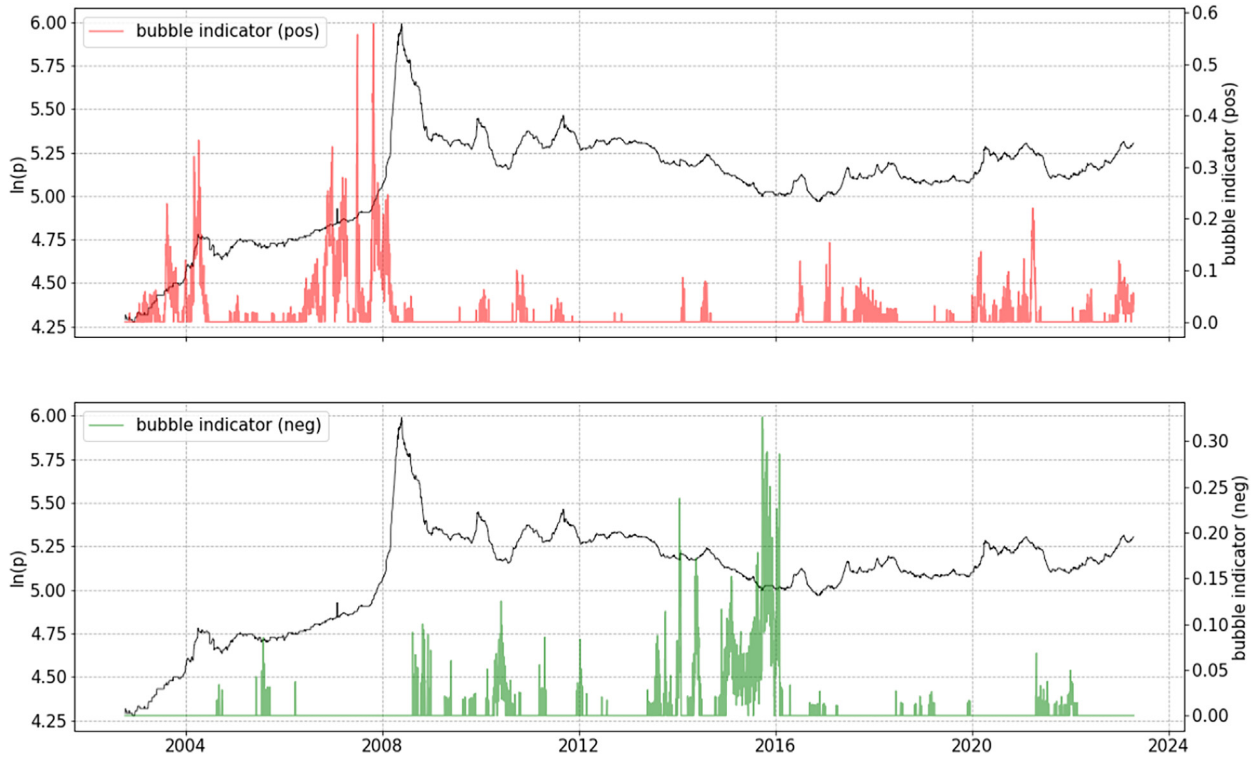

Fig. 5. LPPLS bubble confidence indicators of rice price index.
LPPLS confidence indicators for positive bubbles (upper panel) and negative bubbles (lower panel). The continuous black line indicates the logarithmic price of rice from January 2000 to April 2023; the red one represents a positive bubble indicator, and the green one denotes a negative bubble indicator.

4.1.4. Rice

Fig. 5 shows the bubble status of the rice price index. We identify positive bubble clusters from March 2003 to June 2004, and April 2006 to March 2008. Additionally, we find negative bubble clusters from December 2014 to February 2016, along with a sequence of minor negative bubble clusters from August 2008 to September 2010. Apart from the significant fluctuations during the 2008 financial crisis, the rice price index remains relatively stable. Between 2004 and 2008, the positive bubble signal for rice is particularly robust, intensifying as it approaches the peak of the price index, reaching a maximum value of 0.6. The bursting of the bubble is succeeded by a dense succession of tiny negative bubble signals that are continuously sent out. Following a period of market adjustment, the price index stabilizes, reaching its lowest point in 2016, accompanied by strong signals from negative bubble indicators. In early 2020, the price of rice experiences a 25 % increase, with sustained signals from positive bubble indicators.

Globally, the trading volume of rice is lower than that of maize and wheat. This contributes to the relatively fewer bubbles observed in the rice market. The peak in rice prices during 2007/2008 is influenced by the rising domestic grain prices and limited stocks in several rice-exporting nations. These countries implement export restrictions to protect their domestic rice reserves, which results in a significant portion of rice consumption within their producing countries. For example, China and India collectively account for over 50 % of global rice consumption but engage in limited exports. By July 2008, half of the 22 Asian countries identified by FAO impose export restrictions on rice.

4.1.5. Barley

Fig. 6 illustrates the bubble state of the barley price index. We identify positive bubble clusters from June 2003 to March 2004, June 2007 to April 2008, September 2010 to March 2011, June 2017 to December 2018, and August 2020 to September 2022. Conversely, we observe distinct negative bubble clusters from May 2013 to November 2016, along with a series of minor negative bubble clusters from May 2004 to July 2004, and May 2008 to December 2008. Compared to the other four crops, the barley price index exhibits higher volatility, characterized by more frequent bubble clusters. In 2004, barley prices experience explosive growth owing to poor harvest conditions, with strong positive bubble signals and relatively weaker negative bubble signals. During the 2008 global financial crisis, the barley price index surges from 120 in May 2005 to 370 in October 2007, marking a 208 % increase. Subsequently, following the bubble burst, prices plummet, accompanied by intensive signals from the negative bubble indicators. In 2010, the barley price index surges from 140 in July to 296 in August, registering a 110 % increase within just two months, entering the positive bubble phase. From 2013 to 2016, it experiences a period of instability

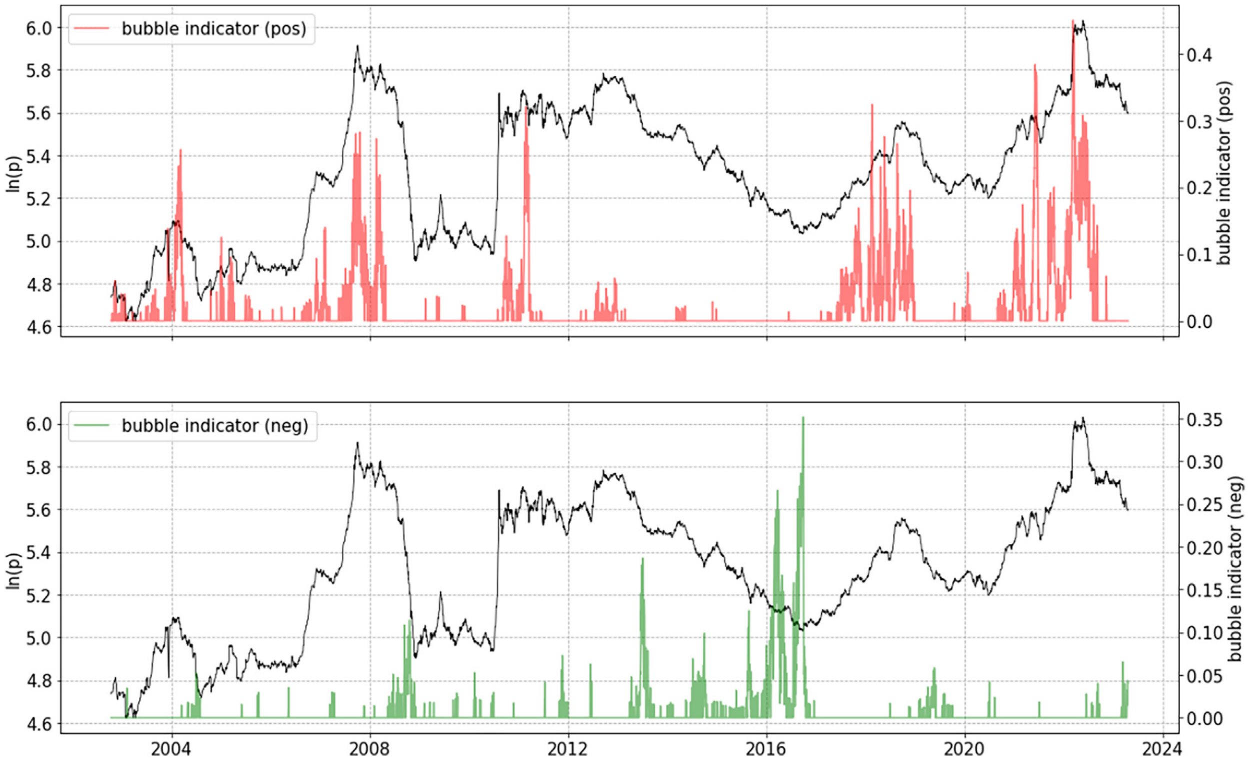

Fig. 6. LPPLS bubble confidence indicators of barley price index.
LPPLS confidence indicators for positive bubbles (upper panel) and negative bubbles (lower panel). The continuous black line indicates the logarithmic price of barley from January 2000 to April 2023; the red one represents a positive bubble indicator, and the green one denotes a negative bubble indicator.

and decline, with prominent negative bubble signals near the bottom. Comparatively, barley's price rebound from February 2017 to December 2018 is substantial, indicating positive bubbling. Additionally, we observe a significant positive bubble trend in the price index from 2020 to 2022, reaching a maximum value of 0.46.

The price bubbles of 2010–2012 and 2020–2022 are both driven by a combination of extreme weather events and regional conflicts. Climatic factors—including natural disasters and meteorological incidents—disrupt food production and supply chains, while regional conflicts, such as civil unrest and geopolitical tensions, further exacerbate these disruptions, impacting food prices. These intertwined factors across different years and regions contribute to fluctuations in global food prices. In 2010, the United States experienced a series of natural disasters, including snowstorms, tornadoes, and droughts, which significantly impacted the production of major agricultural commodities such as wheat, maize, and soybeans. Similarly, Europe suffered diminished wheat and maize production due to Storm Xynthia in the same year. The persistence of La Nina and extreme weather events in 2020 again led to a global surge in food prices. Prolonged La Nina conditions in the United States trigger persistent droughts in the western and southwestern regions, posing the most severe drought threat in a decade. As a major global wheat producer, the drought in the United States significantly impacts wheat yield and quality, causing a major shock in the international agricultural market supply.

Regional conflicts also play a substantial role in the emergence of food price spikes. For instance, the Syrian civil war, which began in 2010, resulted in widespread damage to farmland, leading to a substantial decrease in food production. This imbalance between food supply and demand in the global market caused food prices to surge. Similarly, food price hikes in 2022 are impacted by conflicts such as the Russo-Ukrainian conflict. Russia and Ukraine, the world's largest and fifth-largest wheat exporters, respectively, contribute significantly to global grain exports, providing about 14 % of the world's wheat and 19 % of its barley. However, the conflict and subsequent sanctions imposed by Western countries disrupt their exports, leading to a strain on global grain supplies. Restrictions on crop exports imposed by these and other countries further exacerbate the situation, prompting many governments to regulate crop exports. The resulting scarcity drives up grain prices worldwide. Additionally, factors such as shipping disruptions, increased procurement costs, and uncertainties surrounding Ukraine's upcoming planting season collectively contribute to the most severe shock in the global agricultural market since the 1970s.

Furthermore, the COVID-19 pandemic profoundly affects the agricultural market and is a significant factor contributing to the food crisis in 2020. The pandemic precipitates a sharp increase in unemployment rates, leading to a reduction in income and hindering access to food for many individuals. This escalating challenge in obtaining food further exacerbates global food insecurity. Additionally, the decline in total global merchandise trade caused by border closures and restrictions on the movement of people and goods further disrupts food supply chains.

4.2. Bai-Perron test

To further validate the reliability of the LPPLS confidence indicator, we conduct a Bai-Perron (BP) test on five grain price indices. The BP test, proposed by Bai and Perron (2006), is a method for estimating break dates in time series. It effectively incorporates structural break factors into the traditional unit root test, finding the global minimum of the sum of squared residuals. This algorithm, based on dynamic programming principles, uses least squares to estimate multiple structural breaks and calculate an arbitrary number of breaks.

The BP test is widely used in economics to detect structural breaks in economic time series, signifying points where the deterministic trend changes owing to external shocks in economic development. When analyzing agricultural price bubbles, fluctuations between positive bubbles, negative bubbles, and non-bubble states are influenced by external shocks. Therefore, the transition from bubble to non-bubble states can be considered a structural break component in the development process of agricultural commodities. The BP method is suitable for identifying these breaks in the transition of bubble states. The detected breaks are shown in Table 3.

Based on these breaks, we analyze the bubble indicator values for each of the five agricultural commodities prior to the break dates. Taking wheat as an example, the price index peaks in April 2004. Positive bubble signals are frequently observed in the time interval [2003:11, 2004:04] close to the break date, while negative bubble signals are prevalent in the time interval [2004:07, 2004:08]. From March 2006 to June 2008, the price index surges from 120 to 323, marking a 169 % increase. Positive bubble indicators are frequent in the time interval [2006:04, 2008:04], while negative signals are prominent in the time interval [2008:07, 2008:11]. The LPPLS confidence indicator detects positive bubble characteristics earlier and captures the onset of negative bubbles post-collapse, whereas the BP test result indicates October 2008, lagging behind actual events.

The maize price index surges from 120 in 2005 to a peak of 450 in February 2008, showing a 275 % increase. Positive bubble indicators are consistently present in the time interval [2006:09, 2008:08], while negative bubble indicators start appearing in October 2008 and intensify in December 2008. The BP test identifies October 2008 as the break date, which is delayed from the actual situation. After the maize price index reaches its highest point in 2008 and then plummets, it rebounds again and enters another bubble stage around 2012. From August 2010 to February 2012, positive bubble indicators are frequently observed. During the price decline period, notably in September 2012, negative bubble indicators continue to appear. Similarly, the BP test marks March 2012 as the break date.

The soybean price index peaks in March 2004, with the BP test pinpointing July 2004 as the break date. Before the break date, positive bubble indicators are prevalent in the time interval [2003:05, 2004:06], followed by frequent occurrences of negative bubble indicators in the time interval [2004:08, 2004:10]. Although the BP test results align with the LPPLS model, they slightly lag behind real-time observations.

The rice price index rises from 110 in January 2006 to 400 in May 2008, an increase of 264 %, and then drops to 200 within a year. The BP test identifies January 2008 as the break date. Positive bubble indicators are evident in the time interval [2006:04, 2008:04], while negative bubble indicators persist in the time interval [2006:04, 2008:04]. The results of the BP test closely match those of the LPPLS model.

The barley price index gradually declines from 325 in September 2012 to 154 in August 2016, marking a 53 % decrease, and then begins to rise to 258 in October 2018, an increase of 67 % over 2 years. Subsequent rebounding occurs in 2019, followed by a surge in prices driven by the COVID-19 pandemic in 2020. The BP test takes January 2016 and July 2019 as break dates. Negative bubble indicators frequently issue warnings from 2012 to 2016 before the break date in January 2016. Positive bubble indicators are consistent between 2016 and 2019, and following the break in July 2019, prices continue to rise.

Overall, these findings support the reliability of the LPPLS confidence indicator in detecting significant bubbles in international agricultural prices.

4.3. Markov regime-switching model

As discussed earlier, unpredictable factors such as climate change, regional conflicts, and outbreaks significantly influence the formation of agricultural price bubbles. Uncertainty often leads to short-term supply and demand imbalances in the market, driving up agricultural prices. To confirm this mechanism, we use the geopolitical risk index (GPR) and two climate risk indices as the proxies for uncertainty and employ the Markov regime-switching model to analyze the predictability of

Table 3
Breakpoints of five agricultural commodities.

	Break dates				
wheat	2004:06	2008:10	2012:06	2016:01	2019:07
maize		2008:10	2012:03	2016:02	2019:07
soybeans	2004:07	2008:10	2012:07	2016:04	2019:10
rice	2003:07	2008:01	2011:07		2019:10
barley		2008:09	2012:07	2016:01	2019:07

The determination of the number of breakpoints is carried out using the Sequential method, which involves first testing whether one breakpoint exists. If a breakpoint is found, the test continues in the remaining sample to determine if a second breakpoint exists, and so on. This method gradually increases the number of breakpoints and uses the *F*-test at each step to determine whether to reject the null hypothesis. Sequential *F*-statistics are shown in Appendix A.

uncertainty on agricultural price bubbles. The GPR, developed by Caldara and Iacoviello (2022), is calculated based on the proportion of articles mentioning adverse geopolitical events in major newspapers published in the United States, United Kingdom, and Canada (Baker et al., 2016). The climate physical risk index (PRI) and transition risk index (TRI) are developed by Bua et al. (2024). Leveraging text-based approaches and authoritative sources, the global physical and transition climate risk vocabularies provide a comprehensive, relevance-ranked lexicon of phrases associated with each risk category. Then, the authors calculate the cosine similarity between each daily Reuters news and climate risk vocabularies, generating the "concern" time series that reflect the portion of daily news item discussing physical or transition risk. Finally, the PRI and TRI are the residuals of AR1 processes of the concern series, thus representing innovation/shocks to climate change risks.

Since the price series exhibits two states, bubble and non-bubble, we use a regime-switching model:

$$Ind(t) = \gamma_{0,s_t} + \gamma_{1,s_t} X_{t-1} + \epsilon_t, \tag{14}$$

where $Ind(t)$ signifies the value of the positive and negative bubble indicators, X_{t-1} represents the GPR, PRI and TRI measured at $t-1$, ε_t is the error term, and s_t is a discrete state variable with the value of (0,1), following a two-state Markov process. The transition probability between two states is defined as

$$\begin{aligned} &P(s_t = 1|s_{t-1} = 1) = P_{11}, P(s_t = 2|s_{t-1} = 1) = P_{12}, \\ &P(s_t = 2|s_{t-1} = 2) = P_{22}, P(s_t = 1|s_{t-1} = 2) = P_{21}, \end{aligned} \tag{15}$$

where $P_{ij}\,(i,j = 1,2)$ represents the transition probability of the time series being in state j at time t under the premise that it is in state i at time $t-1$, and the state transition probability matrix is $\begin{pmatrix} P_{11} & P_{12} \\ P_{21} & P_{22} \end{pmatrix}$, with $P_{i1} + P_{i2} = 1$. The state variables govern

Table 4
The predictive ability of geopolitical conflicts, climate physical risk, and climate transition risk on the wheat positive and negative LPPLS confidence bubble indicators.

	Positive bubble		Negative bubble	
	Regime 1 (bubble regime)			
Constant	0.2404***	(0.0037)	0.0633***	(0.0026)
Geopolitical risk index	−0.0029***	(2.9E-5)	0.0002***	(2.34E-5)
Transition risk index	0.1531**	(0.0665)	0.0027	(0.0452)
Physical risk index	−0.1280*	(0.0698)	0.0175	(0.0597)
	Regime 2 (non-bubble regime)			
Constant	0.0039***	(0.0012)	0.0024***	(0.0004)
Geopolitical risk index	3.05E-5***	(1.07E-5)	1.22E-6	(4.10E-6)
Transition risk index	0.0234	(0.0198)	−0.0067	(0.0081)
Physical risk index	0.0407*	(0.0227)	−0.0117	(0.0092)
sigma	0.0283	(0.0003)	0.0120	(0.0001)
AIC	−4.1568		−5.8501	
Log L	9908.430		13940.015	
No. of Obs	4762		4762	

Note: This table reports the estimates from the Markov switching model, with the uncertainty factor using the geopolitical risk index, climate physical risk index, and climate transition risk index as proxies. The numbers in parentheses are the standard errors.
***, **, and * represent significance at 1, 5, and 10 percent, respectively.

Table 5
The predictive ability of geopolitical conflicts, climate physical risk, and climate transition risk on the maize positive and negative LPPLS confidence bubble indicators.

	Positive bubble		Negative bubble	
	Regime 1 (bubble regime)			
Constant	0.2719***	(0.0079)	0.0448***	(0.0013)
Geopolitical risk index	−0.0004***	(5.89E-5)	−2.30E-5**	(1.15E-5)
Transition risk index	0.0379	(0.1076)	0.0798***	(0.0216)
Physical risk index	−0.6013***	(0.1418)	−0.1273***	(0.0242)
	Regime 2 (non-bubble regime)			
Constant	0.0071***	(0.0009)	0.0008***	(0.0002)
Geopolitical risk index	−3.51E-6	(8.28E-6)	−6.79E-7	(1.45E-6)
Transition risk index	0.0229	(0.0164)	−0.0042	(0.0029)
Physical risk index	0.0024	(0.0187)	−0.0058*	(0.0033)
sigma	0.0244	(0.0003)	0.0043	(4.50E-5)
AIC	−4.4839		−7.8490	
Log L	10687.103		18699.476	
No. of Obs	4762		4762	

Table 6
The predictive ability of geopolitical conflicts, climate physical risk, and climate transition risk on the soybeans positive and negative LPPLS confidence bubble indicators.

	Positive bubble		Negative bubble	
	Regime 1 (bubble regime)			
Constant	0.1525***	(2.09E-5)	0.3391***	(0.0045)
Geopolitical risk index	−0.0002***	(2.09E-5)	−0.0008***	(4.22E-5)
Transition risk index	0.0599	(0.0430)	0.2417***	(0.0875)
Physical risk index	−0.1479***	(0.0524)	0.0546	(0.1015)
	Regime 2 (non-bubble regime)			
Constant	0.0045***	(0.0007)	0.0025***	(0.0006)
Geopolitical risk index	−4.96E-6	(5.88E-6)	1.19E-5**	(5.20E-6)
Transition risk index	0.0239**	(0.0115)	−0.0090	(0.0103)
Physical risk index	−0.0034	(0.0133)	−0.0276**	(0.0116)
sigma	0.0165	(0.0002)	0.0156	(0.0002)
AIC	−5.2241		−5.4505	
Log L	12449.463		12988.617	
No. of Obs	4762		4762	

Table 7
The predictive ability of geopolitical conflicts, climate physical risk, and climate transition risk on the rice positive and negative LPPLS confidence bubble indicators.

	Positive bubble		Negative bubble	
	Regime 1 (bubble regime)			
Constant	0.1109***	(0.0074)	0.1275***	(0.0036)
Geopolitical risk index	0.0008***	(8.21E-5)	−1.11E-5**	(5.52E-6)
Transition risk index	0.4295***	(0.1014)	0.0131	(0.0108)
Physical risk index	−0.2307**	(0.1099)	−0.0371***	(0.0122)
	Regime 2 (non-bubble regime)			
Constant	0.0040***	(0.0009)	0.1260***	(0.0033)
Geopolitical risk index	2.67E-5***	(8.23E-6)	−2.88E-5	(2.59E-5)
Transition risk index	0.0126	(0.0165)	−0.1235	(0.0795)
Physical risk index	0.0080	(0.0187)	−0.2480**	(0.1128)
sigma	0.0246	(0.0003)	0.0161	(0.0002)
AIC	−4.4764		−5.2686	
Log L	10669.426		12555.461	
No. of Obs	4762		4762	

the randomness of the state changes in the model structure, while the transition probabilities determine the durability of each regime.

Tables 4-8 report the parameter estimates of the Markov switching model for positive and negative bubble indicators of five agricultural commodities. Examining the results for both positive and negative bubble indicators reveals that the GPR possesses significant predictive power regarding bubbles and crashes in the agricultural market. While the two climate risk indicators show significant predictive power for some agricultural commodity bubbles (e.g., the PRI is significant for maize,

Table 8
The predictive ability of geopolitical conflicts, climate physical risk, and climate transition risk on the barley positive and negative LPPLS confidence bubble indicators.

	Positive bubble		Negative bubble	
	Regime 1 (bubble regime)			
Constant	0.1257***	(0.0029)	0.1450***	(0.0044)
Geopolitical risk index	0.0004***	(1.85E-5)	0.0002***	(3.99E-5)
Transition risk index	0.0148	(0.0632)	0.1107	(0.0784)
Physical risk index	−0.2323***	(0.0662)	1.3833***	(0.0911)
	Regime 2 (non-bubble regime)			
Constant	0.0035***	(0.0012)	0.0034***	(0.0006)
Geopolitical risk index	4.1E-5***	(1.09E-5)	−1.93E-6	(5.07E-6)
Transition risk index	0.0105	(0.0189)	−0.0086	(0.0100)
Physical risk index	0.0098	(0.0214)	−0.0018	(0.0114)
sigma	0.0269	(0.0003)	0.0152	(0.0002)
AIC	−4.2402		−5.4550	
Log L	10106.943		12999.428	
No. of Obs	4762		4762	

rice, and barley, but not for negative bubbles of wheat and soybeans), only the geopolitical risk indicator demonstrates significant predictive ability across all five commodities and for both positive and negative bubbles. This means that even after climate risks are controlled for, geopolitical risk remains a robust and significant predictor of agricultural commodity bubbles. Furthermore, the coefficients of the GPR are all significant in bubble regime, while the vast majority of coefficients are not significant in the non-bubble regime, which indicates that the GPR's predictive power is state-dependent.

5. Conclusions

This study utilizes the LPPLS confidence indicator to diagnose price bubbles in the agricultural market. The LPPLS confidence indicator statistically determines the probability of the current price adhering to bubble characteristics by performing LPPLS fitting on the time series data across numerous time windows at each time point. Applying the LPPLS confidence indicator to five major agricultural price series successfully identifies various bubbles, including the positive bubble triggered by grain production cuts in 2004 and the global financial crisis in 2008, as well as the negative bubble in 2016 and the positive bubble resulting from the COVID-19 pandemic and the Russo-Ukrainian war. Bubble indicators provide early warnings in the early stages of price reversals, with stronger alerts issued closer to the critical point. These bubble periods align with well-known and documented historical events, validating the model's accuracy in detecting bubbles.

To further validate the robustness of the LPPLS confidence indicator, we conduct a Bai-Perron test on the price data, identifying five structural breaks for each food crop. Analyzing the changes in bubble indicator values and price indices before and after these structural breaks reveals shifts in the agricultural market state. Both positive and negative bubble indicators provide strong early warnings for these regime changes, confirming the reliability of the LPPLS confidence indicator. Compared to the Bai-Perron test, the LPPLS confidence indicator offers the advantage of real-time bubble detection and warning, rather than relying on retrospective analysis of the entire sample to identify structural breaks within the period.

Finally, we posit that diverse uncertainties are the primary drivers of bubbles and crashes in food crop prices. Using the GPR as a proxy for uncertainty factors and the LPPLS confidence indicator as a proxy for bubbles, we perform Markov-switching regression. The results demonstrate the robust predictive capability of the GPR for both positive and negative bubble indicators in the bubble regime.

We highlight the finding that the coefficients of the GPR index are significant in the bubble regime but not in the non-bubble regime. This suggests that the predictive power of the GPR index is state-dependent. Agricultural commodities are particularly sensitive to supply shocks owing to their production cycles. Geopolitical events, which often lead to disruptions in the supply chain, can have a profound impact on agricultural prices during bubble regimes when market participants are already concerned about potential scarcities. In bubble regimes, the presence of heightened geopolitical risks can lead to increased speculation and hoarding behavior among market participants, who may anticipate future shortages or price spikes. This can further exacerbate price increases and contribute to the formation and bursting of bubbles in agricultural commodity markets, which in turn affects the predictive power of the GPR index. Geopolitical events can trigger policy responses, such as export restrictions or subsidies, which can significantly influence agricultural commodity prices. During bubble regimes, market participants may anticipate and react to these potential policy changes, further driving the predictive power of the GPR index.

Conversely, in non-bubble regimes, markets are generally characterized by more stable conditions where the impact of geopolitical events on agricultural commodity prices is less pronounced. This could be due to various factors, including a lower level of investor anxiety, or simply a lower level of attention paid to geopolitical risks when market conditions are calmer. As a result, the GPR index, while still capturing real-world events, does not have significant predictive power over market movements in these periods because the market is less responsive to such external shocks.

In summary, practitioners and policymakers must acknowledge that uncertainties such as climate change, regional conflicts, and epidemic outbreaks will likely become more frequent in the future. This underscores the importance of implementing early warning indicators to mitigate losses. Establishing such an indicator for agricultural price bubbles will strengthen national economic stability, ensure food security, safeguard the interests of farmers and investors, and empower the government to craft effective policies and enhance market oversight, reducing potential economic and social risks.

Ethics Statement

Not applicable because this work does not involve the use of animal or human subjects.

CRediT authorship contribution statement

Hai-Chuan Xu: Writing – review & editing, Methodology, Funding acquisition, Conceptualization. **Yu-Zhen Tan:** Writing – original draft. **Han-Xiao Fan:** Writing – original draft, Methodology, Data curation. **Wei-Xing Zhou:** Writing – review & editing, Supervision.

Declaration of competing interest

The authors declare that they have no known competing financial interests or personal relationships that could have appeared to influence the work reported in this paper.

Acknowledgments

We acknowledge financial support from the National Natural Science Foundation of China (71971081, 72171083).

Appendix A. The sequential *F*-statistics of Bai-Perron tests

Table A1
The sequential *F*-statistics of Bai-Perron tests for five agricultural commodities.

	Sequential *F*-statistics				
	wheat	maize	soybeans	rice	barley
0 vs. 1	5972.40*	7888.38*	11018.66*	11726.75*	6427.07*
1 vs. 2	717.49*	973.96*	726.40*	2692.40*	587.19*
2 vs. 3	1865.57*	1424.61*	2027.18*	1386.07*	819.69*
3 vs. 4	235.32*	3829.74*	1280.94*	297.41*	884.51*
4 vs. 5	222.91*	0.00	515.91*	0.00	0.00

*Significant at the 0.05 level.

References

Abreu, D., & Brunnermeier, M. K. (2003). Bubbles and crashes. *Econometrica, 71*, 173–204. https://doi.org/10.1111/1468-0262.00393
Adämmer, P., & Bohl, M. T. (2015). Speculative bubbles in agricultural prices. *Q. Rev. Econ. Finance, 55*, 67–76. https://doi.org/10.1016/j.qref.2014.06.003
Akyildirim, E., Cepni, O., Pham, L., & Uddin, G. S. (2022). How connected is the agricultural commodity market to the news-based investor sentiment? *Energy Econ., 113*, Article 106174. https://doi.org/10.1016/j.eneco.2022.106174
Bai, J., & Perron, P. (2006). *Multiple Structural Change Models: a Simulation Analysis* (pp. 212–238). Cambridge University Press. https://doi.org/10.1017/CBO9781139164863.010
Baker, S. R., Bloom, N., & Davis, S. J. (2016). Measuring economic policy uncertainty. *Q. J. Econ., 131*, 1593–1636. https://doi.org/10.1093/qje/qjw024
Baquedano, F. G. (2015). *Developing an Indicator of Price Anomalies as an Early Warning Tool: A Compound Growth Approach*. Food and Agriculture Organization.
Bartolozzi, M., Drożdż, S., Leinweber, D. B., Speth, J., & Thomas, A. W. (2005). Self-similar log-periodic structures in western stock markets from 2000. *Int. J. Mod. Phys. C, 16*, 1347–1361. https://doi.org/10.1142/S0129183105007972
Basak, S., & Pavlova, A. (2016). A model of financialization of commodities. *J. Finance, 71*, 1511–1556. https://doi.org/10.1111/jofi.12408
Brooks, C., Prokopczuk, M., & Wu, Y. (2015). Booms and busts in commodity markets: bubbles or fundamentals? *J. Futures Mark., 35*, 916–938. https://doi.org/10.1002/fut.21721
Bua, G., Kapp, D., Ramella, F., & Rognone, L. (2024). Transition versus physical climate risk pricing in european financial markets: a text-based approach. *Eur. J. Finance, 30*, 2076–2110. https://doi.org/10.1080/1351847X.2024.2355103
Caldara, D., & Iacoviello, M. (2022). Measuring geopolitical risk. *Am. Econ. Rev., 112*, 1194–1225. https://doi.org/10.1257/aer.20191823
Chen, Z., Yan, B., & Kang, H. (2023). Price bubbles of agricultural commodities: evidence from China's futures market. *Empir. Econ., 64*, 195–222. https://doi.org/10.1007/s00181-022-02254-0
Demirer, R., Demos, G., Gupta, R., & Sornette, D. (2019). On the predictability of stock market bubbles: evidence from lppls confidence multi-scale indicators. *Quant. Finance, 19*, 843–858. https://doi.org/10.1080/14697688.2018.1524154
Demos, G., & Sornette, D. (2017). Birth or burst of financial bubbles: which one is easier to diagnose? *Quant. Finance, 17*, 657–675. https://doi.org/10.1080/14697688.2016.1231417
Etienne, X. L., Irwin, S. H., & Garcia, P. (2014). Bubbles in food commodity markets: four decades of evidence. *J. Int. Money Finance, 42*, 129–155. https://doi.org/10.1016/j.jimonfin.2013.08.008
Etienne, X. L., Irwin, S. H., & Garcia, P. (2015). Price explosiveness, speculation, and grain futures prices. *Am. J. Agric. Econ., 97*, 65–87. https://doi.org/10.1093/ajae/aau069
Fang, M., Lin, Y., & Chang, C. L. (2023). Positive and negative price bubbles of Chinese agricultural commodity futures. *Econ. Anal. Pol., 78*, 456–471. https://doi.org/10.1016/j.eap.2023.03.023
Filimonov, V., Demos, G., & Sornette, D. (2017). Modified profile likelihood inference and interval forecast of the burst of financial bubbles. *Quant. Finance, 17*, 1167–1186. https://doi.org/10.1080/14697688.2016.1276298
Filimonov, V., & Sornette, D. (2013). A stable and robust calibration scheme of the log-periodic power law model. *Phys. Stat. Mech. Appl., 392*, 3698–3707. https://doi.org/10.1016/j.physa.2013.04.012
Gutierrez, L. (2013). Speculative bubbles in agricultural commodity markets. *Eur. Rev. Agric. Econ., 40*, 217–238. https://doi.org/10.1093/erae/jbs017
Hüsler, A., Sornette, D., & Hommes, C. H. (2013). Super-exponential bubbles in lab experiments: evidence for anchoring over-optimistic expectations on price. *J. Econ. Behav. Organ., 92*, 304–316. https://doi.org/10.1016/j.jebo.2013.06.005
Headey, D., & Fan, S. (2008). Anatomy of a crisis: the causes and consequences of surging food prices. *Agric. Econ., 39*, 375–391. https://doi.org/10.1111/j.1574-0862.2008.00345.x
Huang, H., & Xiong, T. (2020). Price bubbles and market integration in global sugar futures markets. *J. Appl. Econ., 23*, 1–20. https://doi.org/10.1080/15140326.2019.1693202

Jiang, Z. Q., Zhou, W. X., Sornette, D., Woodard, R., Bastiaensen, K., & Cauwels, P. (2010). Bubble diagnosis and prediction of the 2005–2007 and 2008–2009 Chinese stock market bubbles. *J. Econ. Behav. Organ., 74*, 149–162. https://doi.org/10.1016/j.jebo.2010.02.007

Johansen, A., Ledoit, O., & Sornette, D. (2000). Crashes as critical points. *Int. J. Theor. Appl. Finance, 3*, 219–255. https://doi.org/10.1142/S0219024900000115

Leiss, M., Nax, H. H., & Sornette, D. (2015). Super-exponential growth expectations and the global financial crisis. *J. Econ. Dynam. Control, 55*, 1–13. https://doi.org/10.1016/j.jedc.2015.03.005

Li, J., Chavas, J. P., Etienne, X. L., & Li, C. (2017). Commodity price bubbles and macroeconomics: evidence from the Chinese agricultural markets. *Agric. Econ., 48*, 755–768. https://doi.org/10.1111/agec.12372

Lin, L., Ren, R. E., & Sornette, D. (2014). The volatility-confined lppl model: a consistent model of 'explosive' financial bubbles with mean-reverting residuals. *Int. Rev. Financ. Anal., 33*, 210–225. https://doi.org/10.1016/j.irfa.2014.02.012

Lux, T. (1995). Herd behaviour, bubbles and crashes. *Econ. J., 105*, 881–896. https://doi.org/10.2307/2235156

Mao, Q., Ren, Y., & Loy, J. P. (2021). Price bubbles in agricultural commodity markets and contributing factors: evidence for corn and soybeans in China. *China Agric. Econ. Rev., 13*, 22–53. https://doi.org/10.1108/CAER-10-2019-0190

Mao, Q., Ren, Y., & Loy, J. P. (2024). Nonlinear price transmission and asynchronous price bubbles: empirical evidence from China's agricultural futures and spot markets. *J. Appl. Econ., 27*, Article 2369441. https://doi.org/10.1080/15140326.2024.2369441

Phillips, P. C., & Magdalinos, T. (2007). Limit theory for moderate deviations from a unit root. *J. Econom., 136*, 115–130. https://doi.org/10.1016/j.jeconom.2005.08.002

Phillips, P. C., Magdalinos, T., & Giraitis, L. (2010). Smoothing local-to-moderate unit root theory. *J. Econom., 158*, 274–279. https://doi.org/10.1016/j.jeconom.2010.01.009

Phillips, P. C. B., Shi, S., & Yu, J. (2015). Testing for multiple bubbles: historical episodes of exuberance and collapse in the s&p 500. *Int. Econ. Rev., 56*, 1043–1078. https://doi.org/10.1111/iere.12132

Phillips, P. C. B., Wu, Y., & Yu, J. (2011). Explosive behavior in the 1990s nasdaq: when did exuberance escalate asset values? *Int. Econ. Rev., 52*, 201–226. https://doi.org/10.1111/j.1468-2354.2010.00625.x

Piesse, J., & Thirtle, C. (2009). Three bubbles and a panic: an explanatory review of recent food commodity price events. *Food Policy, 34*, 119–129. https://doi.org/10.1016/j.foodpol.2009.01.001

Potrykus, M. (2023). Price bubbles in commodity market—a single time series and panel data analysis. *Q. Rev. Econ. Finance, 87*, 110–117. https://doi.org/10.1016/j.qref.2022.12.002

Sanders, D. R., & Irwin, S. H. (2017). Bubbles, froth and facts: another look at the masters hypothesis in commodity futures markets. *J. Agric. Econ., 68*, 345–365. https://doi.org/10.1111/1477-9552.12191

Seyrich, M., & Sornette, D. (2016). Micro-foundation using percolation theory of the finite time singular behavior of the crash hazard rate in a class of rational expectation bubbles. *Int. J. Mod. Phys. C, 27*, Article 1650113. https://doi.org/10.1142/S0129183116501138

Shiller, R. J. (2015). *Irrational Exuberance: Revised and Expanded Third Edition*. Princeton University Press. https://doi.org/10.2307/j.ctt1287kz5

Sornette, D. (2009). *Why Stock Markets Crash: Critical Events in Complex Financial Systems*. Princeton University Press. https://doi.org/10.1515/9781400829552

Sornette, D., & Cauwels, P. (2015). Financial bubbles: mechanisms and diagnostics. *Rev. Behav. Econ., 2*, 279–305. https://doi.org/10.1561/105.00000035

Sornette, D., Demos, G., Zhang, Q., Cauwels, P., & Zhang, Q. (2015). Real-time prediction and post-mortem analysis of the shanghai 2015 stock market bubble and crash. *J. Investment Strateg., 4*, 77–95. https://doi.org/10.21314/JOIS.2015.063

Timmer, C. P. (2010). Reflections on food crises past. *Food Policy, 35*, 1–11. https://doi.org/10.1016/j.foodpol.2009.09.002

Yang, J., Dong, D., Liang, C., & Cao, Y. (2024). Monetary policy uncertainty and the price bubbles in energy markets. *Energy Econ., 133*, Article 107503. https://doi.org/10.1016/j.eneco.2024.107503

Zhi, T., Li, Z., Jiang, Z., Wei, L., & Sornette, D. (2019). Is there a housing bubble in China? *Emerg. Mark. Rev., 39*, 120–132. https://doi.org/10.1016/j.ememar.2019.04.005

Zhou, W. X., & Sornette, D. (2004). Antibubble and prediction of China's stock market and real-estate. *Phys. Stat. Mech. Appl., 337*, 243–268. https://doi.org/10.1016/j.physa.2004.01.051